# *In vitro* bioactivity of titanium-doped Bioglass

Imran M Asif[1], Richard M Shelton[1], Paul R Cooper[1], Owen Addison[1] and Richard A Martin[2]

[1]Biomaterials Unit, School of Dentistry, University of Birmingham, Birmingham, UK

[2]School of Engineering & Applied Science and Aston Research Centre for Healthy Ageing, University of Aston, Aston Triangle, Birmingham, UK.

## Abstract

Previous studies have suggested that incorporating small quantities of titanium dioxide into bioactive glasses may result in an increase in bioactivity and hydroxyapatite formation. The present work therefore investigates the *in vitro* bioactivity of a titanium doped bioglass and compares the results with 45S5 bioglass. Apatite formation was evaluated for bioglass and Ti-bioglass in the presence and absence of foetal calf serum. Scanning electron microscopy (SEM) images were used to evaluate the surface development and energy dispersive X-ray measurements provided information on the elemental ratios. X-ray diffraction spectra confirmed the presence of apatite formation. Cell viability was assessed for bone marrow stromal cells under direct and indirect contact conditions and cell adhesion was assessed using SEM.

## 1. Introduction

Bioactive glasses are of great importance for biomedical applications due to their ability to chemically bond to bone and stimulate new bone growth [1, 2]. Under physiological conditions bioactive glasses dissolve in a controlled manner releasing calcium and phosphorous into solution. Ca and P form an amorphous calcium phosphate layer (ACP) which then crystallizes to form hydroxyapatite (HA) / Hydroxyl-carbonate apatite (HCA) [3, 4] : the naturally occurring mineral present in both teeth and bones.

The archetypal bioactive glass 45S5 Bioglass®, composition $(SiO_2)_{46.1}(CaO)_{26.9}(Na_2O)_{24.4}(P_2O_5)_{2.6}$ mol %, was developed by Larry Hench in 1969 and is now used for a wide range of applications including orthopaedics, cranio-facial and toothpastes [5, 6]. Given the importance of Bioglass® there has been considerable interest in optimising the bioactivity and extending the functionality of these materials. For example, Hill and co-workers have developed Sr based bioactive glasses which are antibacterial, radio-opaque and show a faster rate of HA formation compared with 45S5 Bioglass® [7, 8], Azevedo *et al* and Smith *et al* have developed hypoxic mimicking bioactive glasses containing cobalt and nickel to improve the vascularisation response [9, 10]. Bioactive glasses have also developed with reduced HA formation for soft tissue applications where the presence of HA is undesirable [9].

Recently there have been reports that incorporating titanium into bioactive glasses can improve their bioactivity [11, 12]. Miyata *et al* showed that incorporating $TiO_2$ into sol-gel derived $CaO\text{-}SiO_2$ hybrids results in an increase in HA forming ability [11] whilst Wren *et al* found that incorporating $TiO_2$ into sintered melt quench derived $CaO\text{-}NaO\text{-}SiO_2$ porous bioactive glasses encouraged cell proliferation, particularly when scaffolds containing higher Ti concentrations were used [12]. Titanium is also routinely incorporated into bioactive phosphate glasses to control the solubility and is reported to increase biocompatibility [13-15]. Cell culture studies have shown Ti phosphate microspheres provide a stable surface for cell attachment, growth and proliferation [16]. Wakamura *et al* have also shown that Ti incorporated into HA is bactericidal [17].

The present work therefore explores the effect of incorporating Ti into melt-quenched bioglass. Two compositions were studied, the first composition was 45S5 bioglass, $(SiO_2)_{46.1}(CaO)_{26.9}(Na_2O)_{24.4}(P_2O_5)_{2.6}$, and the second composition was 45S5 bioglass with the addition of 4% $TiO_2$ to yield $(TiO_2)_{3.85}(SiO_2)_{44.3}(CaO)_{25.9}(Na_2O)_{23.45}(P_2O_5)_{2.5}$. This composition was selected for the following reasons: (i) this concentration of $TiO_2$ results in a glass with a $TiO_2$:$SiO_2$ ratio of 0.08:0.92 which is believed to represent the upper limit of titanium incorporation before phase separation occurs [18]; (ii) this level of dopant represents typical levels incorporated (e.g. [9, 10] ) which have been shown to enhance the functionality of bioglass without disrupting the overall glass structure, rate of dissolution and bioactivity; and (iii) this is the only Ti-bioglass composition whose structure has been investigated [19]. This study investigates the surface development and cell response to Ti-doped bioglass compared with 45S5-bioglass. In contrast to some previous studies where glasses are only exposed to a simulated body fluid, SBF, (salt ion solution of 37°C) the impact of proteins on the formation of ACP /HA is taken into specific consideration in these studies. It is known that proteins can adhere to the glass surface thereby inhibiting the dissolution of ions from the glass.

## 2. Method

**2.1. Sample Preparation.** Samples were prepared using standard melt quench techniques [20]. In brief, the melt-quenched glass samples were prepared using $SiO_2$ (Alfa Aesar, 99.5%), $NH_4H_2PO_4$ (Sigma-Aldrich, 99.5%), $CaCO_3$ (Alfa Aesar, 99.95-100.05%), $Na_2CO_3$ (Sigma-Aldrich, 99.5+%) and $TiO_2$ (Sigma-Aldrich, 99.99%). After mixing thoroughly the precursors were placed in a 90% Pt- 10% Rh crucible at room temperature and then heated to 1450°C at a heating rate of 10°C.min$^{-1}$. The melt was then held at 1450°C for 90 minutes before quenching into a pre-heated graphite mould (350°C). Samples were annealed overnight at 350°C before being allowed to cool slowly to room temperature. The compositions of the two glasses prepared were $(SiO_2)_{46.1}(CaO)_{26.9}(Na_2O)_{24.4}(P_2O_5)_{2.6}$ and $(TiO_2)_{3.85}(SiO_2)_{44.3}(CaO)_{25.9}(Na_2O)_{23.45}(P_2O_5)_{2.5}$ and these are labelled 45S5-BG and Ti-BG respectively.

The glass rods (10 mm diameter) were cut into 2mm thick discs using a low speed diamond saw (Isomet, Buehler, USA) with an ethanol based lubricant Dp-blue (Struers, Denmark) to minimise aqueous contact. Discs were ground and polished using a DAP-7 polishing machine (Struers, Denmark) using a series of silicon carbide papers (P800, P1000, P1200, P2400 and P4000) and Dp-blue as a lubricant, followed by a final polish using 0.06 micron colloidal silica. Following the grinding and polishing protocol the discs were cleaned in acetone for 10 minutes using an ultrasonic bath to remove any debris that may have adhered during polishing before air drying for 20 minutes in a laminar flow hood. Prior to undertaking the experiments the discs were sterilised using dry heat at 160°C for 2 hours. Samples were stored in a desiccator between stages of preparation to reduce exposure to atmospheric moisture.

**2.2. Surface evolution.** Immersion experiments were conducted using two types of media: (i) a protein free Alpha Modified Eagles Medium (αMEM) culture media supplemented with 2.5% 1M HEPES, 1% penicillin/streptomycin and (ii) an αMEM media with 10% Foetal Calf Serum (FCS) to provide a supply of proteins. All the constituents of the culture medium were purchased from Sigma Aldrich, UK. Sterilised 45S5-BG and Ti-BG discs were immersed in 20ml of αMEM culture medium with and without the addition of FCS and incubated at 37°C in an atmosphere of 5% $CO_2$ for periods of time ranging from 1 hour to 7 days. After immersion the discs were rinsed with acetone (99.9%) twice to terminate the surface reactions before air drying in laminar flow hood. Experiments were performed in triplicate.

Following immersion the surface development was studied using a Carl Zeiss EVO MA10 scanning electron microscope (SEM) operating at 10kV. The bioactive glass discs were mounted onto SEM stubs using conductive copper tape and splutter coated with gold. Compositional analysis of the bioactive glass surfaces was undertaken using an Energy Dispersive X-ray (EDX) spectroscopy detector (PentaFET Precision, INCAx-act, OXFORD instruments) operating at 20kV. Three discs were analysed for each time period and a minimum of five measurements were undertaken per disc, including a control sample, for SEM and EDX experiments. X-ray diffraction (XRD) spectra were collected using a Rigaku *SmartLab* Diffractometer operating with an incident wavelength of 1.54 Å.

### 2.3. Cell culture

Wistar rat bone marrow stromal cells [21] (BMSCs), passage 0, were culture in 75cm$^2$ flasks containing 15ml of 10% FCS supplemented αMEM (sαMEM) culture medium and incubated in a humidified atmosphere at 37°C with 5% $CO_2$. Discs of 45S5-BG, Ti-BG and glass cover slips (control) were placed in a 24-well plate and covered with 2ml of sαMEM. BMSCs were seeded onto the glass discs with a seeding density of 1 x $10^4$ cells and incubated at 37°C with 5% $CO_2$ for five different time periods ranging from 2-14 days to determine the cell viability growth curve. Culture medium was replaced every two to three days and all the experiments were repeated in triplicate. Following incubation after 2, 5, 8, 12 and 14 days the culture medium was removed and stored for pH testing. Cell viability and proliferation studies were undertaken for cells in both direct and indirect contact with the glass. Attached cells were detached using 0.25% trypsin-EDTA solution. Cell viability was determined using the Trypan blue dye exclusion assay.

Alizarin Red S staining was used to detect the presence of calcium deposits on the bioactive glass surface. BMSCs cultured on 45S5-BG, Ti-BG and glass coverslips (control) for 14 days were fixed using buffered formalin (10%) for 30 minutes and stained with Alizarin Red S staining solution (pH 4.2). Cells were washed with phosphate buffered solution (PBS) (Sigma Aldrich) and viewed using a transmission light microscope (Nikon Eclipse TE300).

Quantitative analysis of cell growth and morphology were undertaken using SEM. BMSCs cultured on 45S5-BG, Ti-BG and glass coverslips (control) for 7, 10 and 14 days were fixed using 2% gluteraldehyde in 0.1M sodium cacodylate buffer (pH 7.4) for 1 hour. The samples were then dehydrated using a graded series of ethanol from 10% ethanol to 100 % ethanol, each for 10 minutes. 95% and 100% ethanol were repeated twice for a further 10 minutes to ensure complete dehydration. Hexamethyldisilazane (HDMS) was added for 30 minutes and then removed to allow the samples to be coated with gold for SEM imaging.

## 3. Results and Discussion

SEM images for 45S5-BG and Ti-BG with and without the presence of 10% FCS are shown in Figures 1-4 respectively. Surface formation was evident for 45S5-BG after 1 hour and full coverage was observed by 6 hours (Fig. 1). The Ti-BG exhibits slower formation of ACP /HA compared with 45S5-BG (Fig. 2). Minimal formation was observed for Ti-BG after 1 hour and at 6 hours the ACP /HA coverage on Ti-BG was similar to coverage observed after only 1 hour for 45S5-BG. Similarly the formation observed after 24 hours for Ti-BG was comparable with the formation present after only 6 hours for the 45S5-BG. A similar trend was observed for 45S5-BG and Ti-BG immersed in αMEM with 10% FCS where the ACP /HA layer forms faster for the 45S5-BG (Fig. 3) compared with Ti-BG (Fig. 4).

Termination of the surface reaction using acetone caused dehydration and cracking of the apatite layer. This became more evident for samples immersed in αMEM for longer time periods. Thicker formations resulted in larger facets following dehydration. Rinsing

and drying protocols were kept constant for all samples. The average facet areas for 45S5-BG were ~ 840, 2100, 4500 and 18000 $\mu m^2$ after immersing for 1, 6, 24 and 96 hours respectively which are shown in Figure 5. As shown the largest facets were observed for the 45S5-BG without FCS and this trend was repeated at all time points. Initially the same trend was observed between 45S5-BG and Ti-BG in the presence of 10% FCS. However as time increased the difference between facet sizes reduces and by 7 days the observed difference was minimal. This suggested that the reduction in ACP/HA formation under conditions more representative of *in vivo* where proteins are present may be minimal.

The surface elemental ratios determined by EDX are given in Figures 6 and 7. The deposited surface layer was composed of calcium and phosphorous and at 21 days the Ca/P ratio for the 45S5-BG without proteins (Fig 6a) was 1.58 which was indicative of apatite where values in the range 1.5 to 1.7 are commonly reported [22]. The concentration trend observed was broadly the same for all samples. Initially a rapid drop in the concentration of sodium was observed as it dissolved into the surrounding media; this was consistent with bioactivity models where the first step is the ion exchange of the cation $Na^+$ from the glass with $H^+$ from the surrounding physiological fluid [23, 24]. The concentration of calcium and phosphorous are also shown to drop initially although at a slower rate. This resulted in a silica-rich phase as the remaining ions (Na, Ca and P) dissolved more rapidly from the bioactive glass surface.

At six hours the concentration of Si reached a maximum and then decreased as a function of time whilst the levels of Ca and P increase, this was attributed to the formation of an amorphous calcium phosphate / hydroxyapatite surface layer. As the ACP/ HA forms the X-rays were unable to penetrate into the bulk bioactive glass and the corresponding Si signal associated with the bulk glass is reduced. Note, at 20keV the linear attenuation coefficient of HA is ~ $1.95x10^3$ $cm^{-1}$ [25], consequently the incident X-ray beam will fall to 1/e of its incident intensity within 5 microns of the incident surface. It is evident that the formation of ACP /HA was more rapid for 45S5-BG in the absence of FCS (Fig. 6a), the concentration of Si drops an order of magnitude between 6 hours and 4 days and was almost negligible after 7 days. The addition of Ti was found to retard the formation of ACP /HA as shown in Fig. 7a. The concentration of Si decreased by only a factor of ~2 between 6 hours and 4 days as the concentrations of Ca and P rise due to the formation of ACP /HA. Interestingly the concentration of Ti did not decrease during the formation of surface ACP /HA and actually increases during the first 24 hours before reaching a plateau. This demonstrated that the Ti ions after dissolving from the Ti-BG were then incorporated onto the surface layer either as a Ti-phosphate or Ti-substituted HA. The formation of Ti-substituted HA has previously been reported [17, 26, 27]. Ti(IV) is believed to substitute Ca and not P within HA. Given the ionic radius of $Ti^{4+}$ (0.605 Å) is greater than that of $P^{5+}$ (0.38 Å) but less than that of $Ca^{2+}$ (1.00 Å) [28] it is likely that Ti substitutes Ca sites. Wakamura *et al* [17] suggested that Ti(IV) exists in the HA crystals as divalent cations such as $[Ti(OH)_2]^{2+}$ and $[TiHPO_4]^{2+}$ which may explain why the Ca/P ratio was relatively low (~1.2) after the Ti-BG was immersed in media for 4 and 7 days (Fig. 7a). Allowing for the substituted Ti the revised ratio (Ca+Ti)/P of ~1.7 was closer to typical HA values. As shown in Figure 6(a/b) the fall in Si concentration was significantly slower when FCS was present. This indicated that the formation of HA was retarded for 45S5-BG due to the presence of proteins. Previously studies have observed similar trends for bioglass in simulated body fluid containing proteins [29] and these results are consistent with our observation of smaller HA facets. The addition of FCS to Ti-BG was found to have a negligible impact on the evolution of surface composition. This supports the previous observation that the variation in facet size, which was related to the thickness of HA, was not significantly effected for Ti-BG bioglass with or without the presence of proteins. An initial starting ratio of Ti/(Ca+Ti) of 0.13 was present in the as prepared Ti-BG compared

with the optimal bactericidal ratio reported 0.1 [17]. However after 7 days in media the deposited surface layer had a Ti/(Ca+Ti) ratio of 0.26. This data suggested that Ti is either preferentially incorporated into HA or formed a phase separated Ti-phosphate layer.

The reduction in ACP /HA formation for the protein free samples is in contrast to previous studies for Ti-doped sol-gel derived bioactive glasses which was also undertaken in a protein free environment with SBF [11]. This difference may be attributed to the very high concentration of –OH groups typically present in sol-gel systems which can result in glasses that dissolve very rapidly, therefore the addition of Ti which reduced the dissolution may help to provide a stable platform for the HA to form. In the present system the addition of Ti also reduced the solubility however this was undesirable in melt quench glasses which typically dissolve at a much slower rate. Notably, other studies of Ti-doped bioglass do not report HA formation [12]. However, the data presented here is in agreement when proteins are incorporated into the media. The concentration of silicon (detected from the bulk glass) is significantly lower for Ti-BG compared to the 45S5 when proteins are added (Fig. 6b and Fig. 7b). This indicates a thicker surface formation on Ti-BG compared to 45S5.

XRD spectra on the surface formation layer for 45S5-BG and Ti-BG, after incubating at 37°C for 96 hours in (protein free) Alpha Modified Eagles Medium, are shown in Figure 8. The formation of a hydroxyapatite like layer is clearly evident for both samples [30]. The Ti-BG spectrum is sharper indicating a higher degree of crystallisation. In contrast the main peak ~ 32° for the 45S5 bioglass still shows evidence of the underlying amorphous calcium phosphate layer which is known to be present prior to crystallisation.

Figure 9 shows the number of viable cells as a function of time for 45S5-BG, Ti-BG and control. As shown there was no statistical difference in the number of viable cells between 45S5-BG and Ti-BG samples in direct contact with the exception of a single measurement point at 12 days. In contrast for indirect contact there were significantly more viable cells present for 45S5-BG compared with the Ti-BG after 8, 12 and 14 days. No significant differences in cell viability between control, 45S5-BG and Ti-BG were observed at any of the time points studied ($p>0.05$). Wren *et al* [12] reported an increase in cell viability upon the addition of $TiO_2$, whilst the current study identified a negligible difference for direct contact experiments and a decrease for indirect contact. The difference in these results may be attributed to the higher level of porosity reported by Wren *et al*; it is therefore possible that the increased surface area compensated for the lower rates of dissolution.

Figure 10 shows the resultant pH level after the glasses were immersed in BMSC culture for up to 14 days. 45S5-BG and Ti-BG both exhibited a rapid rise in pH to ~ 8.8 before slowly decreasing to a value of ~ 7.8 after 14 days. In comparison the pH never rises above 7.6 ± 0.1 for the control samples. The observed pH values were marginally higher for 45S5-BG compared with Ti-BG for all samples but this difference was only statistically significant ($p<0.05$) at 2 and 5 days indicating that 45S5-BG dissolved more rapidly during the first 5 days. As the glass dissolved it released sodium ions and the pH rises accordingly. These results were consistent with the earlier observation where the concentration of Na was found to fall at a much slower rate for Ti-BG compared with 45S5-BG (Figures 6 and 7) which also indicated that the 45S5-BG dissolved more rapidly.

Figure 11 illustrates the Alizarin red staining after 14 days in BMSC culture. Staining is apparent for both the 45S5-BG (a) and Ti-BG (b) samples. The bottom right corner shows the calcium containing glass samples whilst the solid dark band shows the high concentration of calcium ions during the formation of an ACP / HA layer. A smaller amount of staining is seen in the media (top right of both images) illustrating that calcium ions are present in the media prior to precipitating onto the glass surface. SEM images of the BMSC growth after culturing for 10 days on the bioactive glass surfaces is shown in Figure 12 and it is clear that the cells have not attached to the Ti-BG.

## Conclusions

Previous work has suggested that incorporating Ti into bioactive silicate based glasses may be advantageous and result in an increase in cell proliferation and hydroxyapatite formation. The results presented here show that the addition of 4% $TiO_2$ into 45S5-BG reduces the rate of ACP/HA formation under protein-free media conditions. However under more physiological conditions, with the addition of proteins, an increase in HA formation was observed. Ti was found to be preferentially incorporated into the ACP / HA surface layer at the expense of Ca and the resultant surface formation was more crystalline in nature. 45S5-BG and Ti-BG both supported cell proliferation; a similar number of viable cells were observed when in direct contact with the glass. Under indirect contact conditions cell viability was higher for 45S5-BG. Cell attachment was however significantly reduced for Ti-BG. It is concluded that incorporating 4% $TiO_2$ into 45S5-BG whilst supporting bioactivity, apatite formation and cell viability it is not ideal for cell adhesion. Further work is needed to determine if incorporating Ti into melt quench derived silicate glasses can have the same beneficial effect reported in other bioactive glass systems. Substituting Ti directly for Si within these glasses rather may help maintain the desired dissolution rate.

## References


[1] Hench LL, Splinter, R. J., Allen, W. C. and Greenlee, T. K. Bonding mechanisms at the interface of ceramic prosthetic materials. Journal of Biomedical Materials Research Symposium 1971;5:25.

[2] Clark AE, Hench LL, Paschall HA. Influence of Surface Chemistry on Implant Interface Histology - Theoretical Basis for Implant Materials Selection. Journal of Biomedical Materials Research 1976;10:161-74.

[3] Skipper LJ, Sowrey FE, Pickup DM, Drake KO, Smith ME, Saravanapavan P, et al. The structure of a bioactive calcia-silica sol-gel glass. Journal of Materials Chemistry 2005;15:2369-74.

[4] Martin RA, Twyman H, Qiu D, Knowles JC, Newport RJ. A study of the formation of amorphous calcium phosphate and hydroxyapatite on melt quenched Bioglass using surface sensitive shallow angle X-ray diffraction. Journal of Materials Science-Materials in Medicine 2009;20:883-8.

[5] Hench LL. The story of Bioglass (R). Journal of Materials Science-Materials in Medicine 2006;17:967-78.

[6] Hench LL, Day DE, Höland W, Rheinberger VM. Glass and Medicine. International Journal of Applied Glass Science 2010;1:104-17.

[7] Fredholm YC, Karpukhina N, Brauer DS, Jones JR, Law RV, Hill RG. Influence of strontium for calcium substitution in bioactive glasses on degradation, ion release and apatite formation. Journal of The Royal Society Interface 2012;9:880-9.

[8] Martin RA, Twyman HL, Rees GJ, Barney ER, Moss RM, Smith JM, et al. An examination of the calcium and strontium site distribution in bioactive glasses through isomorphic neutron diffraction, X-ray diffraction, EXAFS and multinuclear solid state NMR. Journal of Materials Chemistry 2012;22:22212-23.

[9] Azevedo MM, Jell G, O'Donnell MD, Law RV, Hill RG, Stevens MM. Synthesis and characterization of hypoxia-mimicking bioactive glasses for skeletal regeneration. Journal of Materials Chemistry 2010;20:8854-64.

[10] Smith JM, Martin RA, Cuello GJ, Newport RJ. Structural characterisation of hypoxia-mimicking bioactive glasses. J Mat Chem B 2013;1:1296-303.

[11] Miyata N, Fuke K, Chen Q, Kawashita M, Kokubo T, Nakamura T. Apatite-forming ability and mechanical properties of PTMO-modified CaO-SiO2-TiO2 hybrids derived from sol-gel processing. Biomaterials 2004;25:1-7.

[12] Wren AW, Coughlan A, Smale KE, Misture ST, Mahon BP, Clarkin OM, et al. Fabrication of CaO-NaO-SiO2/TiO2 scaffolds for surgical applications. Journal of Materials Science-Materials in Medicine 2012;23:2881-91.

[13] Abou Neel EA, Chrzanowski W, Knowles JC. Effect of increasing titanium dioxide content on bulk and surface properties of phosphate-based glasses. Acta Biomaterialia 2008;4:523-34.
[14] Moss RM, Abou Neel EA, Pickup DM, Twyman HL, Martin RA, Henson MD, et al. The effect of zinc and titanium on the structure of calcium-sodium phosphate based glass. Journal of Non-Crystalline Solids 2010;356:1319-24.
[15] Abou Neel EA, Mizoguchi T, Ito M, Bitar M, Salih V, Knowles JC. In vitro bioactivity and gene expression by cells cultured on titanium dioxide doped phosphate-based glasses. Biomaterials 2007;28:2967-77.
[16] Lakhkar NJ, Park J-H, Mordan NJ, Salih V, Wall IB, Kim H-W, et al. Titanium phosphate glass microspheres for bone tissue engineering. Acta Biomaterialia 2012;8:4181-90.
[17] Wakamura M, Hashimoto K, Watanabe T. Photocatalysis by Calcium Hydroxyapatite Modified with Ti(IV): Albumin Decomposition and Bactericidal Effect. Langmuir 2003;19:3428-31.
[18] Pickup DM, Sowrey FE, Newport RJ, Gunawidjaja PN, Drake KO, Smith ME. The structure of TiO2-SiO2 sol-gel glasses from neutron diffraction with isotopic substitution of titanium and O-17 and Ti-49 solid-state NMR with isotopic enrichment. J Phys Chem B 2004;108:10872-80.
[19] Martin RA, Moss RM, lakhkar NJ, Knowles J, cuello GJ, Smith ME, et al. Structural characterization of titanium-doped Bioglass using isotopic substitution neutron diffraction. Physical Chemistry Chemical Physics 2012;14:15807.
[20] Martin RA, Twyman HL, Rees GJ, Smith JM, Barney ER, Smith ME, et al. A structural investigation of the alkali metal site distribution within bioactive glass using neutron diffraction and multinuclear solid state NMR. Physical Chemistry Chemical Physics 2012;14:12105-13.
[21] Wang L, Shelton RM, Cooper PR, Lawson M, Triffitt JT, Barralet JE. Evaluation of sodium alginate for bone marrow cell tissue engineering. Biomaterials 2003;24:3475-81.
[22] Raynaud S, Champion E, Bernache-Assollant D, Thomas P. Calcium phosphate apatites with variable Ca/P atomic ratio I. Synthesis, characterisation and thermal stability of powders. Biomaterials 2002;23:1065-72.
[23] Saravanapavan P, Jones JR, Pryce RS, Hench LL. Bioactivity of gel-glass powders in the CaO-SiO2 system: A comparison with ternary (CaO-P2O5-SiO2) and quaternary glasses (SiO2-CaO-P2O5-Na2O). Journal of Biomedical Materials Research Part A 2003;66A:110-9.
[24] Martin RA, Yue S, Hanna JV, Lee PD, Newport RJ, Smith ME, et al. Characterizing the hierarchical structures of bioactive sol-gel silicate glass and hybrid scaffolds for bone regeneration. Philosophical Transactions of the Royal Society a-Mathematical Physical and Engineering Sciences 2012;370:1422-43.
[25] http://physics.nist.gov/PhysRefData/FFast/html/form.html.
[26] Yin S, Ellis DE. First-principles investigations of Ti-substituted hydroxyapatite electronic structure. Physical Chemistry Chemical Physics 2010;12:156-63.
[27] Huang J, Best SM, Bonfield W, Buckland T. Development and characterization of titanium-containing hydroxyapatite for medical applications. Acta Biomaterialia 2010;6:241-9.
[28] Shannon R. Revised effective ionic radii and systematic studies of interatomic distances in halides and chalcogenides. Acta Crystallographica Section A 1976;32:751-67.
[29] Mei J, Shelton RM, Marquis PM. Changes in the elemental composition of Bioglass during its surface development in the presence or absence of proteins. Journal of Materials Science: Materials in Medicine 1995;6:703-7.
[30] Elliott JC, Mackie PE, Young RA. Monoclinic hydroxyapatite. Science 1973;180:1055-7.

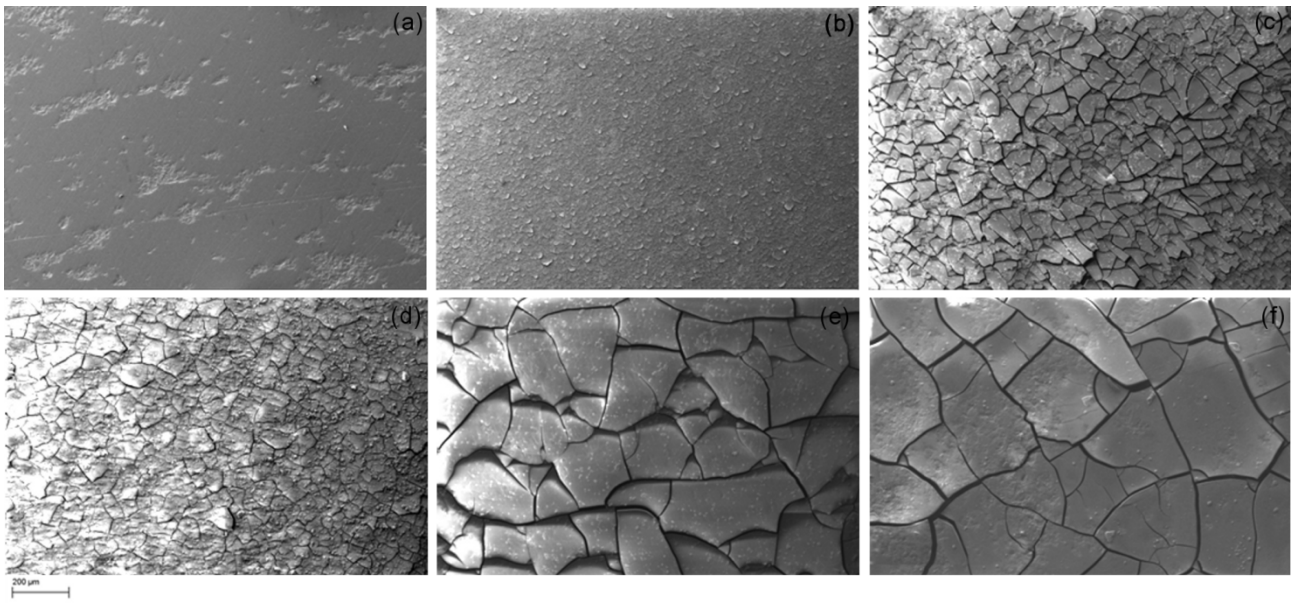


Fig1

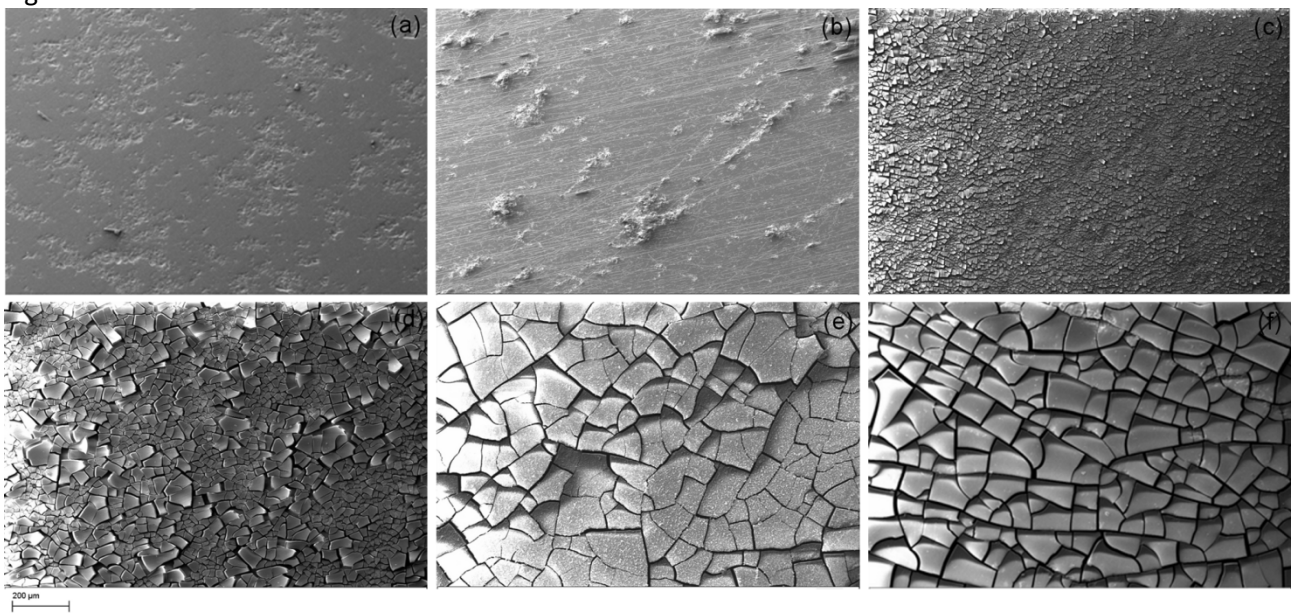


Fig 2

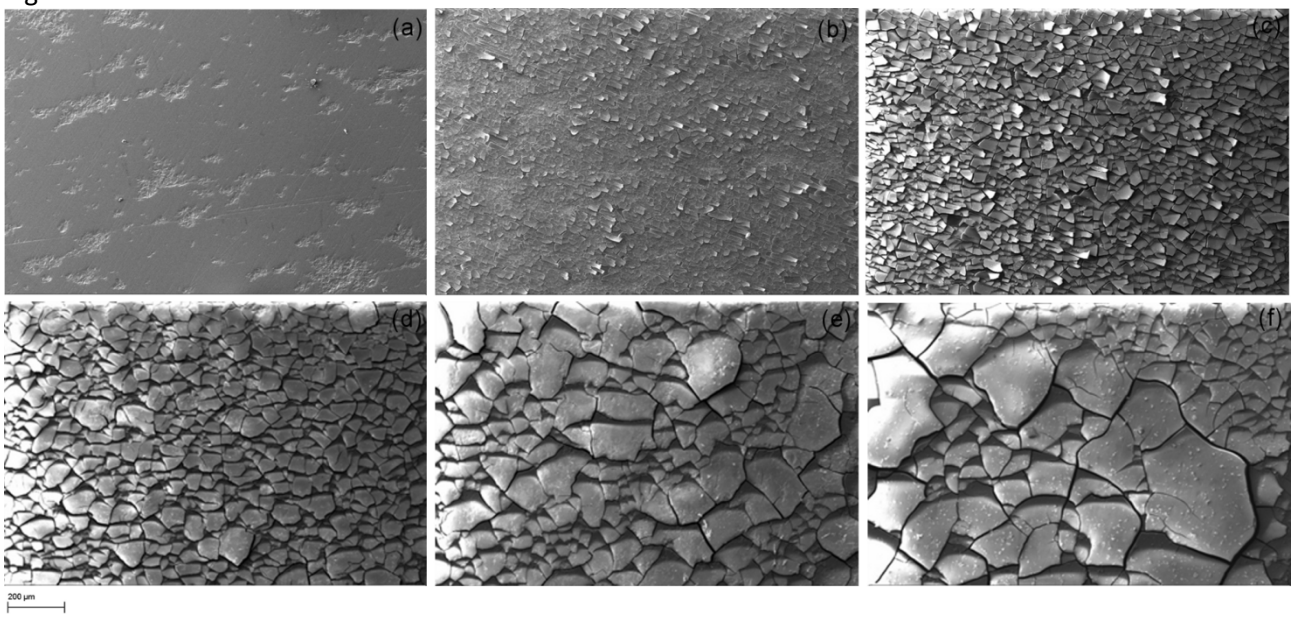


Fig3

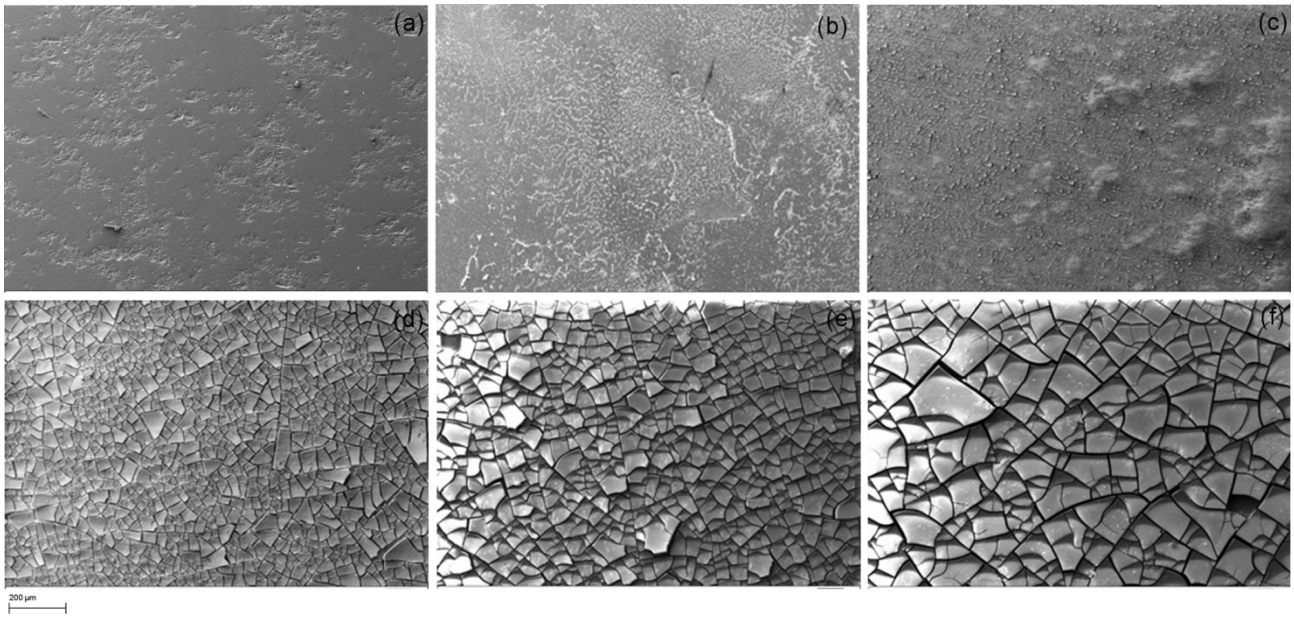


Fig4

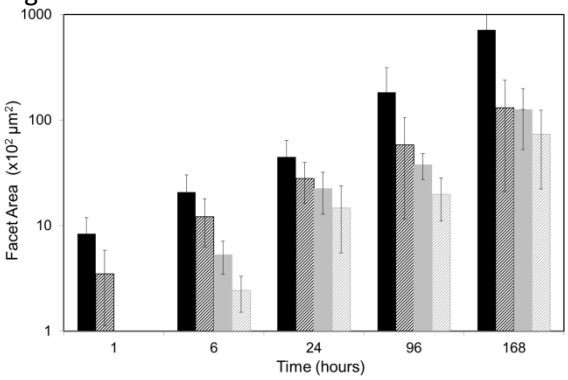


Fig 5

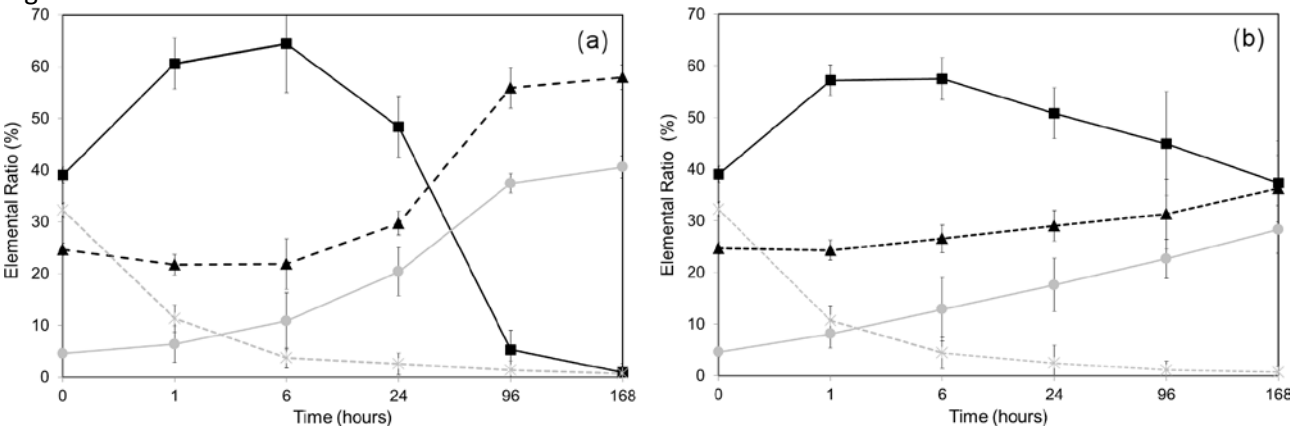


Fig 6 (a) and (b)

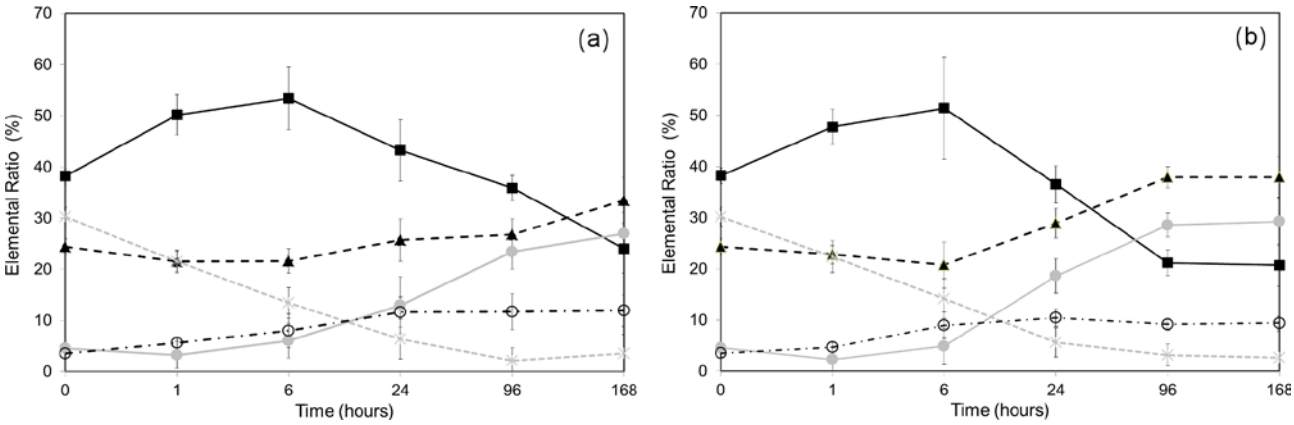


Fig 7 (a) and (b)

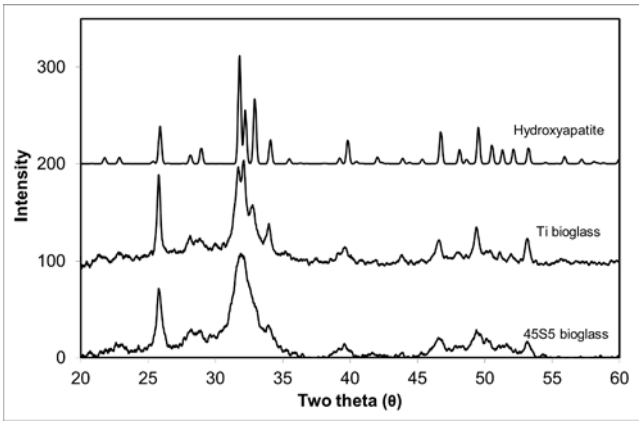


Fig 8

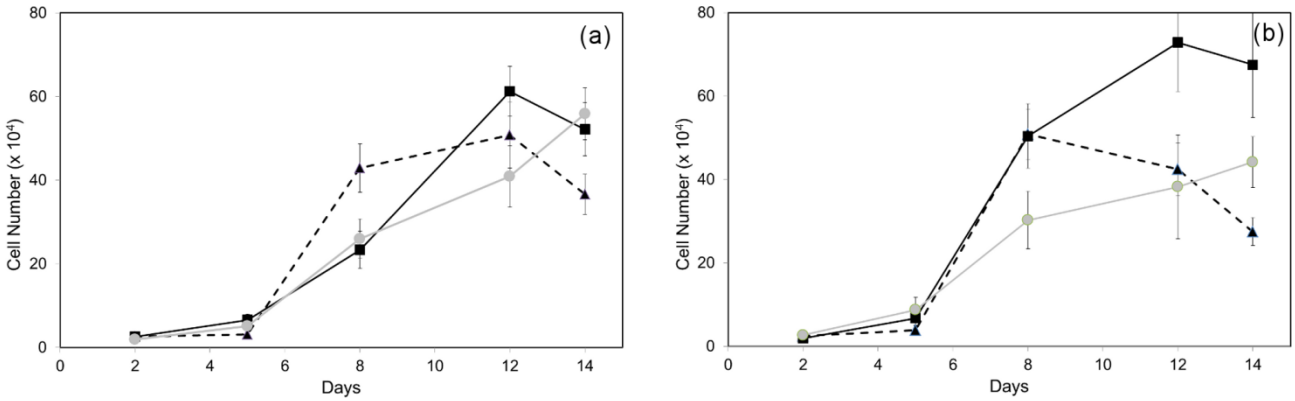


Fig 9 (a) and (b)

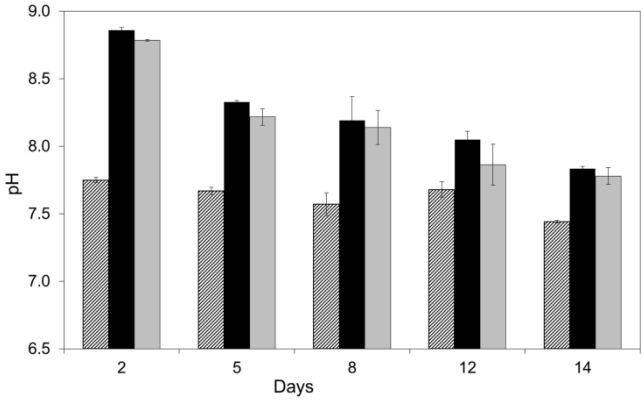


Fig 10

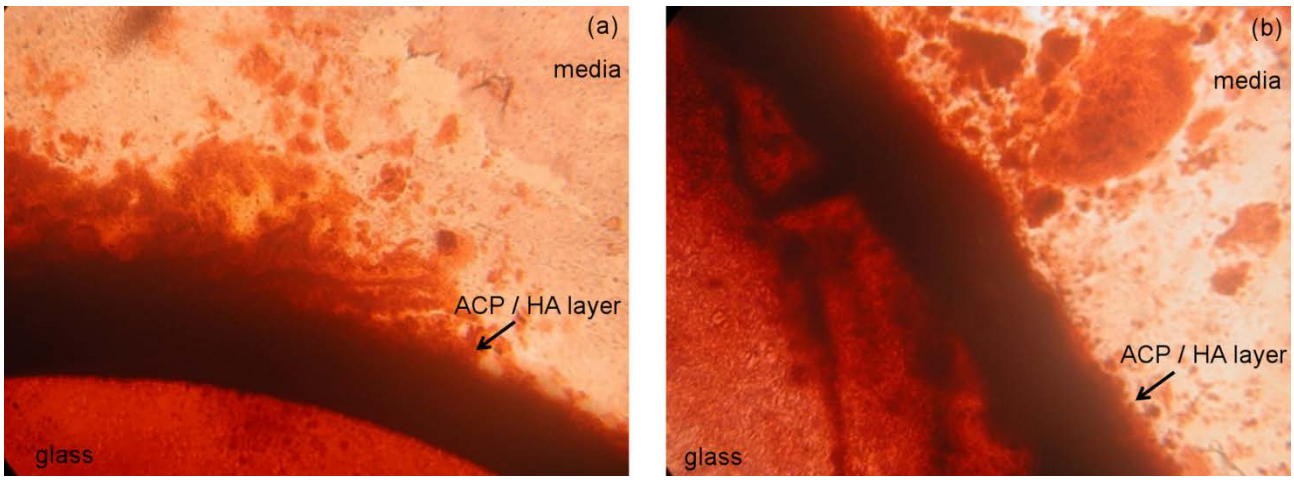


Fig 11

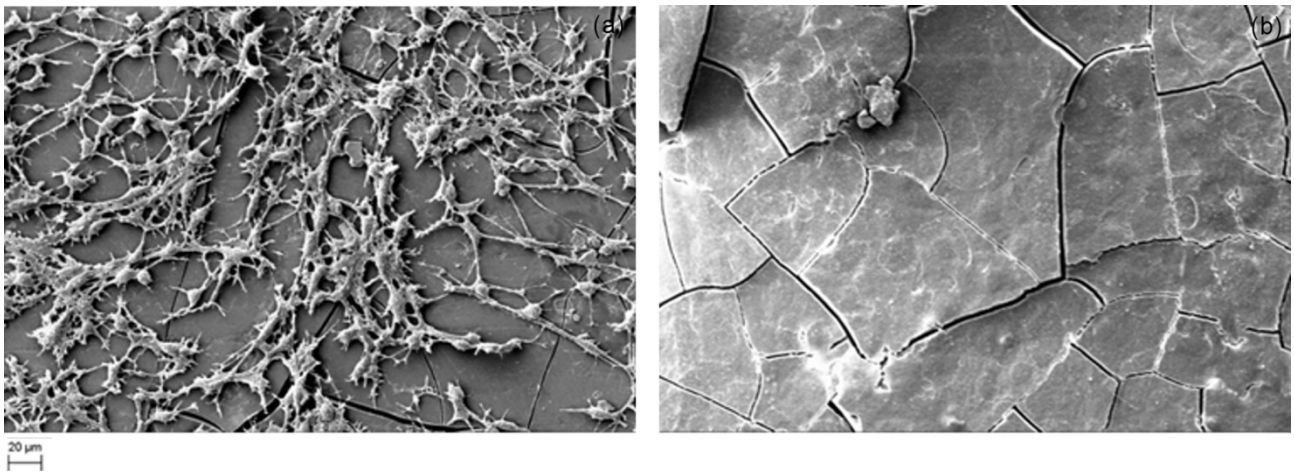


Fig 12

Figure Captions

Figure 1. SEM micrographs of 45S5-BG showing the formation of an ACP / apatite surface layer after immersing in αMEM for 0, 1, 6, 24, 96 and 168 hours (a-f) respectively.

Figure 2. SEM micrographs of Ti-BG showing the formation of an ACP / apatite surface layer after immersing in αMEM for 0, 1, 6, 24, 96 and 168 hours (a-f) respectively.

Figure 3. SEM micrographs of 45S5-BG showing the formation of an ACP / apatite surface layer after immersing in αMEM with 10% FCS for 0, 1, 6, 24, 96 and 168 hours (a-f) respectively.

Figure 4. SEM micrographs of Ti-BG showing the formation of an ACP / apatite surface layer after immersing in αMEM with 10% FCS for 0, 1, 6, 24, 96 and 168 hours (a-f) respectively.

Figure 5. Average area of the HA surface facets as a function of time for the 45S5-BG and Ti-BG bioactive glass with and without the presence of FCS. The facet formation is indicative of the thickness of ACP/ apatite surface formation. Left to right: ■45S5-BG; ◪45S5-BG+FCS; ■ Ti-BG; ◪ Ti-BG + FCS.

Figure 6. Surface elemental ratio (%) determined by EDX as a function of time for (a) 45S5 without proteins and (b) 45S5 with 10% FCS. Illustrating the change in elemental ratio as the glass dissolves and an ACP/ apatite surface layer forms. ■ Si; ▲ Ca; ● P; X Na.

Figure 7. Surface elemental ratio (%) determined by EDX as a function of time for (a) Ti-45S5 without proteins and (b) Ti-45S5 with 10% FCS. Illustrating the change in elemental ratio as the glass dissolves and an ACP/ HA surface layer forms. ■ Si; ▲ Ca; ● P; X Na, ○ Ti.

Figure 8. XRD spectra for 45S5-BG and Ti-BG. Monoclinic hydroxyapatite is given as a reference standard [30].

Figure 9. Number of viable BMSC cells following (a) direct contact and (b) indirect contact culture: ■ 45S5-BG; ▲ control; ● Ti-BG.

Figure 10. pH of media resulting from bioactive glasses placed in αMEM culture with BMSCs. Left to right: ◪ control glass; ■ 45S5-BG; ■ Ti-BG.

Figure 11. Alizarin red staining after 14 days in BMSC culture of 45S5-BG (a) and Ti-BG (b). The staining shows the background level of calcium present in the glass with a significantly enhanced concentration at the glass surface.

Figure 12. SEM images of BMSC cultures after 10 days on 45S5-BG (a) and Ti-BG (b).